29th International Congress on Sound and Vibration
The annual congress of the International Institute of Acoustics and Vibration (IIAV)
9–13 July 2023
ICSV29

Annual Congress of the International Institute of Acoustics and Vibration (IIAV)

# EXPERIMENTAL INVESTIGATION OF INFLOW-DISTORTION-INDUCED TONAL NOISE IN A SUB-SONIC FAN TEST RIG

Lukas Klähn, Luciano Caldas, Robert Meyer, Antoine Moreau and Ulf Tapken
*German Aerospace Center (DLR), Institute of Propulsion Technology, Engine Acoustics Department*
*e-mail: lukas.klaehn@dlr.de*

Experimental investigation on the influence of inflow distortions on fan noise was performed at the low-speed Co-/Counter Rotating Acoustic Fan Test rig (CRAFT). The investigated fan stage is designed such that the dominant interaction modes at the first and second BPF are excited weakly in upstream direction, but strongly in downstream direction, due to the mode propagation angle. Two major tonal source mechanisms are described in the literature and addressed in this work. The first mechanism is the inflow-distortion-rotor interaction, which can generate high sound power levels at the blade passing frequencies at high blade tip mach numbers or low rotor blade counts. For the measurements performed this source seems to be relevant only for extreme inflow distortion cases. The second mechanism is linked to the modulation of the rotor-stator interaction (RSI), which is caused by the periodically fluctuating incidence angle and the resulting fluctuation of the rotor wakes shape. The sources distorted phase and amplitude lead to a less effective constructive interference of the conventional interaction modes and a less a destructive interference of the adjacent modes. As consequence, a broader mode spectrum is propagating to the measurement sections. The overall sound power level for our specific fan stage can be more than 7 dB higher or 1 dB lower than the baseline, depending on the inflow distortion profile and BPF harmonic.

## 1. Introduction

In order to deepen our understanding of the fan noise generation mechanisms due to inflow distortion, aeroacoustic experiments were performed at the low-speed fan test facility CRAFT [1]. The investigated fan stage is designed in such a way that the excited RSI mode is cut-on at the blade passing frequency (BPF) [2]. However, at BPF the interaction mode has a propagation angle almost parallel to the stator blade chord in upstream direction and almost normal to the stator blade chord in downstream direction. This leads to a weak excitation of the mode propagating in upstream direction and a strong excitation of the respective mode propagating in downstream direction, caused by the dipole characteristic of the source. The same is true for the interaction mode at 2 BPF. By proficient choice of rotor and stator blade numbers this effect can be utilized for a low-noise fan design [3].

In this work we investigate the influence of distorted mean flow profiles on the tonal noise emission of this fan stage. Manifold future aircraft designs are comprising boundary layer ingestion [4] or distributed propulsion [5] in both concepts the fans may face strong inflow distortions. The tonal noise is affected by two mechanisms. First, the interaction of the mean inflow profile with the rotor results in the periodic fluctuations of the rotor forces, which in turn excites tonal noise at specific modal structures [6, 7]. Second, the tonal RSI noise is also modulated by the periodic changes of the rotor wakes, which may lead to additional excited modes, as shown by means of numerical simulations [8, 9]. However, this periodic changes in the rotor wakes may also cause a less effective excitation of the dominant modes, leading to a reduction of the overall tonal noise [10].

The non-axisymmetric inflow profile was generated with the help of perforated plates combined with a honeycomb structure mounted inside the channel upstream the fan. The effects on broadband noise of these experiments were investigated in a previous study [11, 12]. More details about the test setup, instrumentation, and inflow distortions tested are given in Section 3. The theory on fan tonal noise excitation is discussed in Section 2. Experimental results are presented and discussed in Section 4 and 5. Section 6 finishes this paper with conclusions and remarks.

## 2. Theoretical background on tonal fan noise due to inflow distortions

Conventional fans generate tonal noise at the blade passing frequency and its harmonics. The underlying mechanism is the periodic interaction of the rotor wakes with the stator vanes leading edge. Due to the fixed phase relations of the sources on the stator leading edges, only a few specific azimuthal modes (Tyler-Sofrin modes) are excited under axisymmetric inflow conditions at the BPF and its harmonics [2]. The azimuthal mode order of these interaction modes are given by:

$$m_{\text{TS}} = (-)hB + kV \,,\; k \in \mathbb{Z} \,, \tag{1}$$

where $h$ is the harmonic order, $B$ the blade count, and $V$ the vane count. The CRAFT rotor rotates in the negative direction in the used coordinate system, as indicated by the the negative sign.

### 2.1 Distorted-inflow-rotor interaction

In order to analyze the correlation between the mean flow profile and the tonal noise excitation, the mean flow profile is decomposed into circumferential harmonics of the order $\mu$ by means of a discrete Fourier transform (DFT):

$$U_x(r,\theta) = \sum_{\mu=-\infty}^{\infty} u_x(\mu, r) e^{j\mu\theta} \,. \tag{2}$$

In this work a radial average of the mean flow harmonics is used:

$$\overline{u}_x(\mu) = \frac{1}{R^2} \int_0^R u_x(\mu, r)\, r\, dr \,. \tag{3}$$

Tonal noise is generated due to the interaction of the inflow distortion with the rotor. The mechanism can be described as a generalized Tyler-Sofrin theory [6, 7]. The excited azimuthal mode orders are given by:

$$m_{\text{BLI}} = kB + \mu \,,\; k \in \mathbb{Z} \,. \tag{4}$$

### 2.2 Impact of distorted inflow on rotor-stator interaction

The RSI tonal noise is affected by the inflow distortion, such that the phase relations between the sources on the stator leading edge are out of tune. While the interference pattern under axisymmetric inflow conditions is, in theory, perfectly in phase (constructive for Tyler-Sofrin Modes and destructive otherwise). Th non-axisymmetric inflow leads to a broader mode spectrum as the Tyler-Sofrin modes are not perfectly constructive interfering while the adjacent modes are interfering less destructive. The hypothesis assumed in this work is that the excited modes in the rotor stator interaction correlate in the mode order with the Tyler-Sofrin mode, that is shifted by the mean flow harmonic [8, 9]:

$$m_{\mathrm{RSI},\mu} = (-)hB + kV + \mu. \tag{5}$$

The correlation between the amplitudes of the acoustic modes of azimuthal order $m_{\mathrm{RSI},\mu}$ and the amplitude of the corresponding mean flow harmonic $u_x(\mu)$ has been investigated only with numerical methods to our knowledge. This study shall support the development of an theoretical formulation of the underlying mechanisms, i.e. a formulation of the shift in phase and amplitude of the sources, based on the mean flow harmonics.

## 3. Description of the test rig, inflow distortions, and instrumentation

Experiments were performed at the low-speed fan test facility CRAFT. A sketch of the test rig is shown in Fig. 1. The tested reference fan stage consists of a $453.6\,\mathrm{mm}$ in diameter, $B = 18$ bladed rotor, and a $V = 21$ stator vanes. The maximum fan speed is $\eta = 4500$ rpm and the flow rate is adjusted with a conic throttling device installed at the rig's exhaust. Acoustic measurements were performed with in-duct wall flush mounted microphone arrays, which allows the decomposition of the modal structure into its azimuthal and radial constituents. The arrays consist of a rotating (traverse) axial microphone array with 30 uniformly spaced sensors, $23.75\,\mathrm{mm}$ apart in the inlet section, and 22 sensors with the same spacing in the outlet section. Measurements were performed at 59 uniformly spaced circumferential positions, with $10\,\mathrm{s}$ sample length and a sampling frequency of $65\,536\,\mathrm{Hz}$.

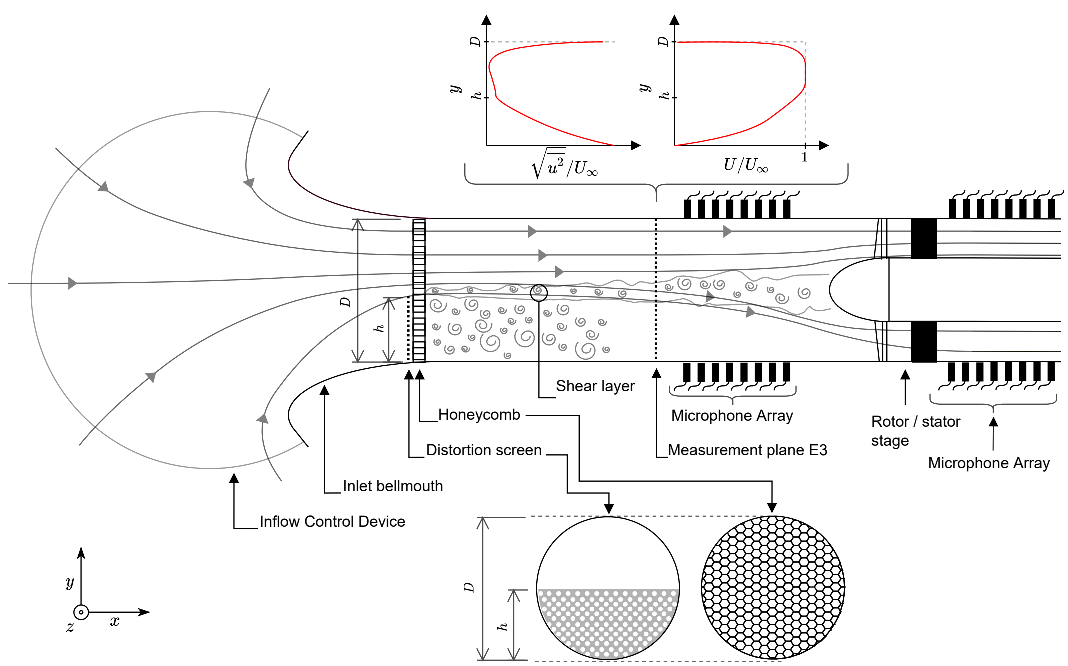


Figure 1: Sketch of the measurement section of the CRAFT for the investigation of inflow distortions. Figure extracted and edited from [11].

For the investigation of inflow-distortion induced tonal fan noise three distortion screens with a variation in fence height (FH) in % of duct diameter and open area ratio (OR) in % are investigated, as in Fig. 2. The distortion screens used were not specifically designed for these tests. Instead, they are used to investigate fundamental relations between the distorted mean inflow profile and the fan tonal noise. The

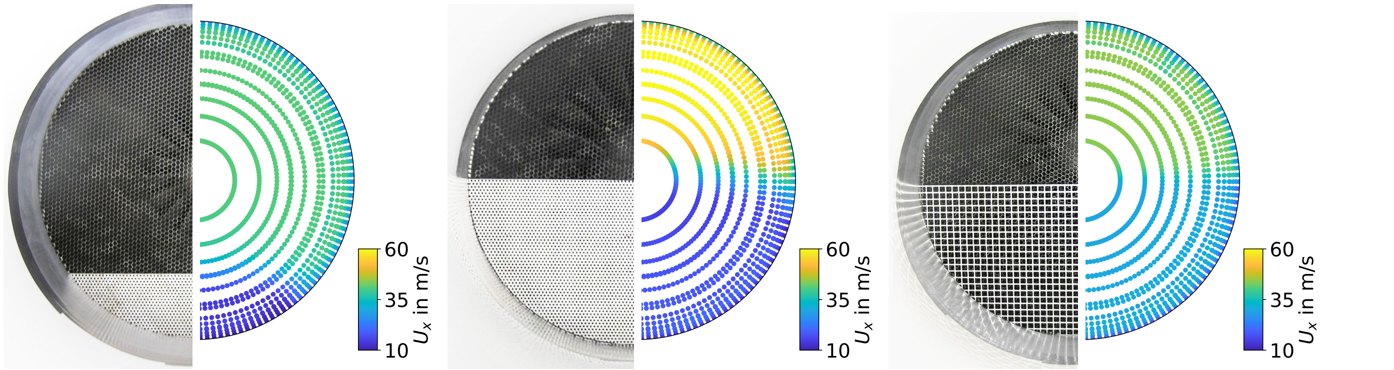


Figure 2: Inflow distortion screens and resulting mean flow profiles from left to right: FH20-OR33, FH50-OR33, FH50-OR64.

inflow distortion screens were mounted on a honeycomb structure $1220\,\mathrm{mm}$ upstream of the rotor leading edge. The aerodynamic measurement plane is located $670\,\mathrm{mm}$ upstream of the rotor leading edge. In Fig. 2 the velocity profiles are shown, as measured by total pressure rakes mounted in a circumferential traverse at every $2.5^{\circ}$ and scaled to the operating point of the acoustic measurements. We ensured with measurements at 2250 rpm and 4500 rpm shaft speed that the velocity profiles are virtually independent of the mean flow velocity. The mean flow distribution was decomposed into circumferential harmonics that can be correlated with the measured mode orders. A uniform and low turbulence levels inflow is ensured by an inflow control device (ICD) mounted on the rig's inlet. Further information about the test rig and instrumentation capabilities are found in [1].

## 4. Azimuthal mean flow decomposition

On the left-hand side of Fig. 3 the radial average of the mean flow harmonics are compared for the different profiles. The velocities are scaled to match the operating point of the acoustic measurements. As the results of the DFT are symmetric, only the positive side of spectrum is shown.

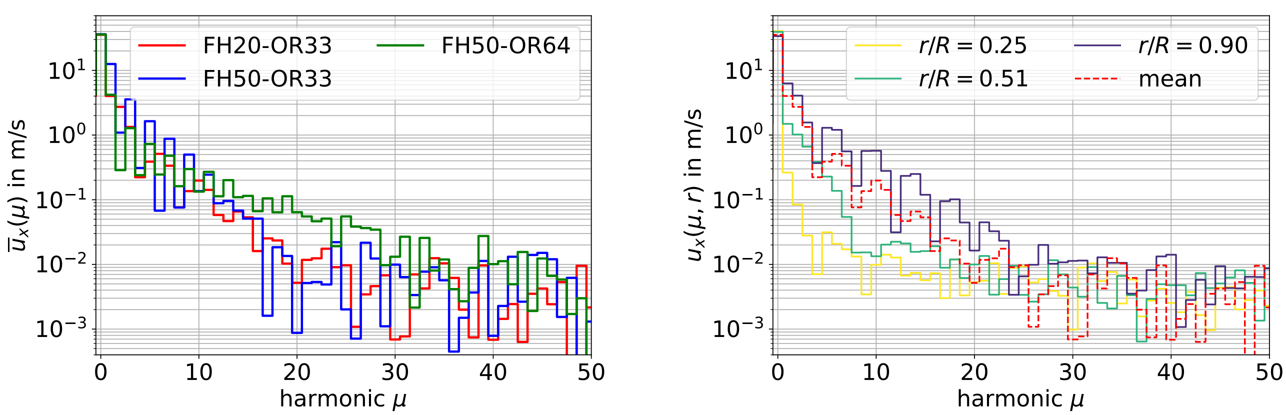


Figure 3: Azimuthal DFT of the mean flow profiles. Left: radial average of the three different inflow distortion profiles. Right: DFT result at three radial positions for FH20-OR33.

All Profiles have the highest distortion at the first harmonic. The profile FH20-OR33 has also relatively high portions at the harmonics 2 and 3 while the profiles with fence height 50 have higher portions at odd orders (3, 5, 7). Note that the profile FH50-OR64 shows the strongest distortion at mid to high harmonic orders between $\mu = 12$ and $\mu = 33$.

On the right-hand side plot in Fig. 3 the mean flow harmonics for the profile FH20-OR33 are shown at three radial positions, as well as the radial average. It is obvious that the harmonic orders differ significantly at the different radii. While almost no distortion is present at the small radius, it is very strong closer to the casing. Kobayashi and Groeneweg [6] perform a decomposition into Bessel functions to take the radial velocity profile into account, allowing to predict radial orders of the excited acoustic modes. As a first estimate, we use the radial average for the comparison with the azimuthal acoustic mode orders.

## 5. Azimuthal mode spectra at the BPF and higher harmonics

Acoustic measurements were performed five different flow rates $\Phi$ and three rotor speeds. In this work results for the design operating condition of the CRAFT reference fan at $\eta = 4500$ rpm and $\Phi = 0.33$ are presented. The mass flow (and in turn the flow coefficient) was adjusted by correlating the pressure rake measurements shown in Fig. 2 with a single pitot probe that was present in the inlet during the acoustic measurements. The fan speed and mass flow were normalized to sea-level standard atmosphere conditions as defined by the ICAO. The microphone data were resampled using a rotor trigger to compensate variations in the rotation speed. The rotor locked data were then used to perform the radial mode analysis (RMA) of the BPF tones [13]. The RMA results of the first 4 BPF harmonics are depicted in Fig. 4 - 6 for the different inflow distortions compared to the baseline case (black crosses) where only the honeycomb structure was installed in the inlet channel. The computed sound powers of all propagating radial modes were summed to obtain the azimuthal sound power levels $\text{PWL}_m$. Note that in the RMA is based on the assumtion of a constant mean flow. However, the distorted mean flow causes a distortion of the eigenfunctions and axial wavenumbers of the acoustic modes, especially for upstream propagating modes with low azimuthal and radial mode orders [14]. This refraction of the modal wave-fronts leads to distorted mapping onto the azimuthal modes, which is not considered in this study and has to be taken into account when interpreting the results.

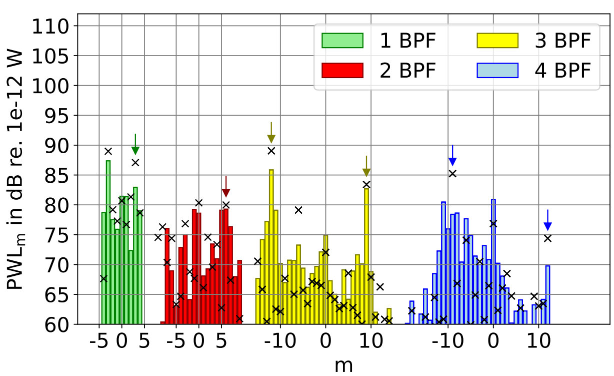


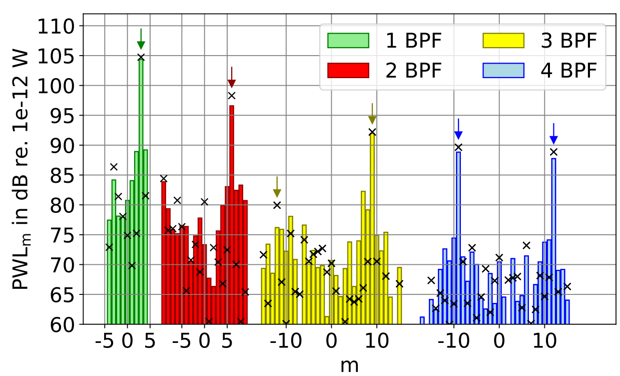


Figure 4: Left: Azimuthal mode powers of upstream propagating modes for the FH20-OR33 configuration at fan operating point: $\eta = 4500$ rpm and $\Phi = 0.33$, right: downstream propagating modes in the outlet.

In the left plot of Fig. 4, the upstream propagating modes for the modes radiated upstream in the inlet are shown for the distortion FH20-OR33. The Tyler-Sofrin (TS) modes (marked by arrows) are generally decreased by the distortion, while the adjacent modes are increased. In particular, this is found for the negative azimuthal mode orders for 3 BPF and 4 BPF around the respective TS-mode. These modes are co-rotating with the rotor. The downstream propagating TS-modes are not much affected in this case (Fig. 4 right). The modes around the TS modes are, however, elevated. Note that the TS mode at 1 BPF

($m = 3$) is not strong in the upstream emitted sound field, but very dominant in the downstream emitted sound field. The same effect is observed for TS-mode at 2 BPF ($m = 6$). As was described above, this results from themodes propagation angle [3].

In Fig. 5 the results for the strongest distortion FH33-OR50 are shown. The TS modes are drastically reduced, except for the BPF upstream. In the downstream propagating sound field, the adjacent modes to the TS modes show the highest amplitude. We understand this mode spectrum as a result of the modulation of the rotor wakes. For the upstream propagating sound field, we see an increase of a wide range of modes that may also result from an interaction of the rotor with the mean flow distortion.

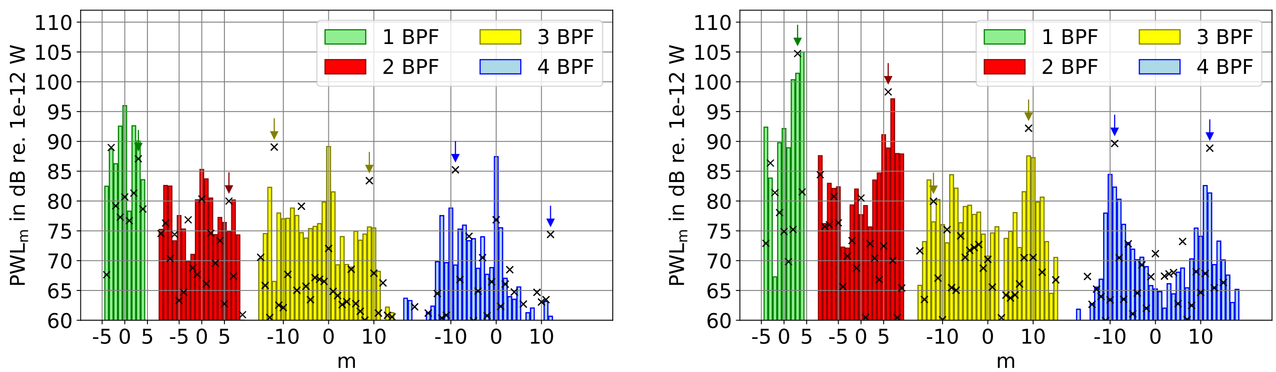


Figure 5: Left: Azimuthal mode powers of upstream propagating modes for the FH50-OR33 configuration at fan operating point: $\eta = 4500$ rpm and $\Phi = 0.33$, right: downstream propagating modes in the outlet.

Fig. 6 shows the FH50-OR64 inflow distortion. At BPF the sound power level is increased significantly, in particular in the inlet. Generally speaking, the co-rotating modes are more strongly increased which would be plausible if the sound source was driven by the interaction of the inflow distortion with the rotor.

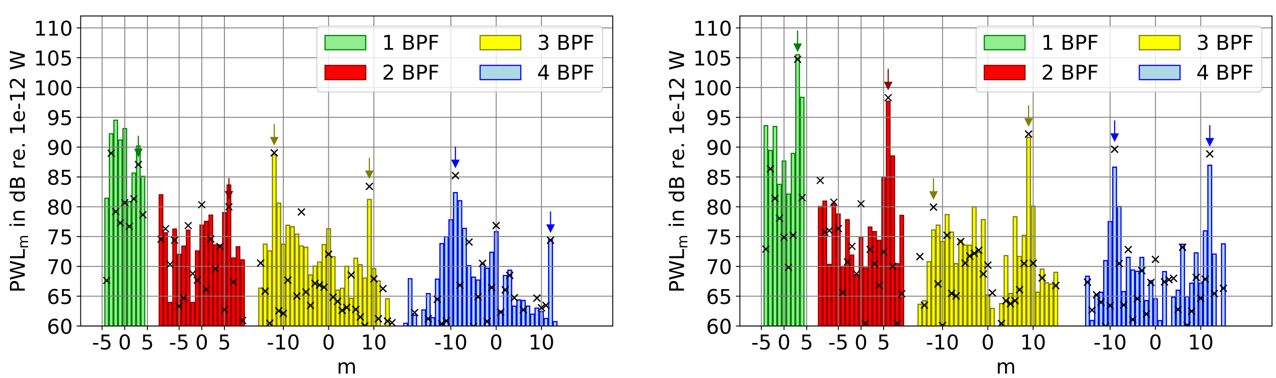


Figure 6: Left: Azimuthal mode powers of upstream propagating modes for the FH50-OR64configuration at fan operating point: $\eta = 4500$ rpm and $\Phi = 0.33$, right: downstream propagating modes in the outlet.

In order to find general trends, the modal sound power levels are summarized into three measures: The summed sound power of all Tyler-Sofrin modes, the overall sound power at that frequency and the residual sound power, i.e. all modes that are not TS-modes. The results are shown in Fig. 7 for the sound power levels of the upstream propagating modes in the inlet. As the TS mode is not effectively excited for the BPF and 2 BPF, the elevation of the adjacent modes has a very strong influence on the overall sound power of up to 7 dB for the FH50 cases. The 3 and 4 BPF show a decrease of the TS modes and an increase of the residual modes sound power. The overall sound power is actually reduced at 3 BPF in the FH20-OR33 case.

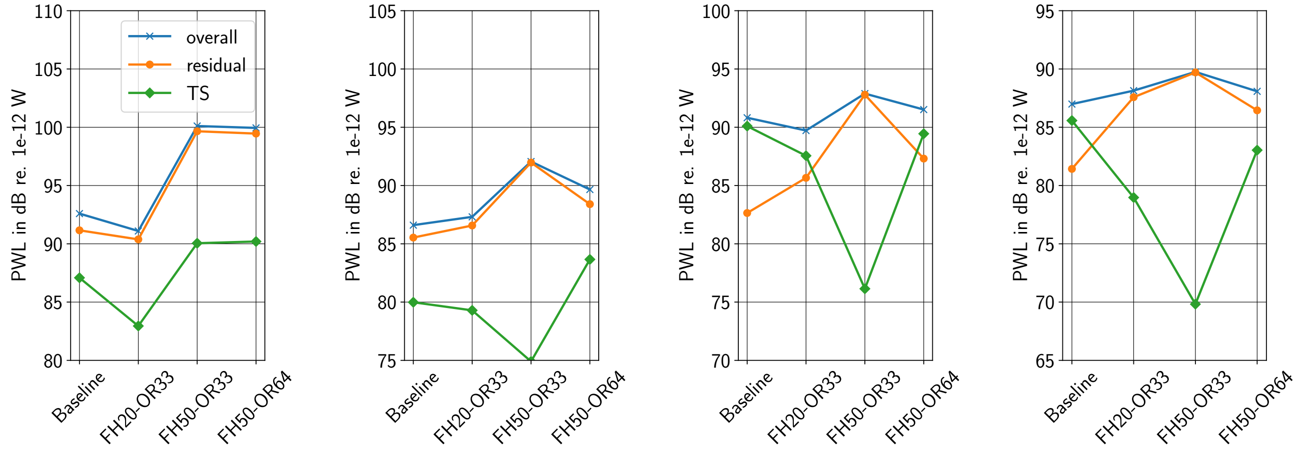


(a) BPF (b) 2 BPF (c) 3 BPF (d) 4 BPF

Figure 7: Sound power of blade tones emitted upstream for the operating point $\eta = 4500$ rpm and $\Phi = 0.33$.

In Fig. 8 the downstream sound power levels are shown. The results are similar to the upstream case at 3 BPF and 4 BPF: The TS mode is decreased by the inflow distortion, while the residual modes are increased. The overall sum is not as strongly affected as for the upstream propagation. In some cases the overall sound power is reduced when the inflow distortion is present.

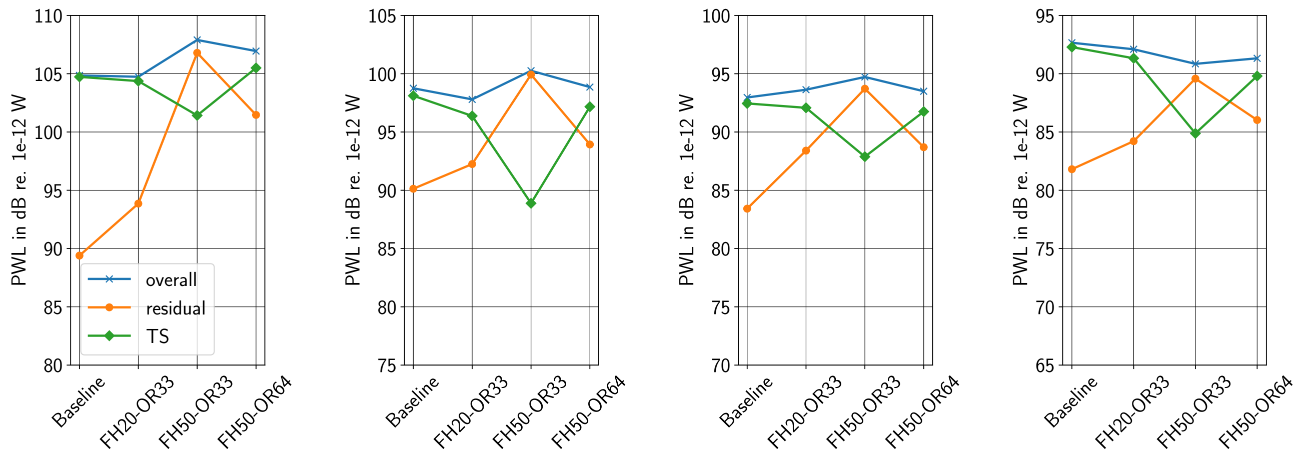


(a) BPF (b) 2 BPF (c) 3 BPF (d) 4 BPF

Figure 8: Sound power of blade tones emitted downstream for the operating point $\eta = 4500$ rpm and $\Phi = 0.33$.

The inflow distortion FH20-OR33 affects the tonal noise emission the least. The mean flow harmonics for this case are distributed rather smooth across the first three higher harmonics. While the other profiles are dominated by specific harmonics.

## 6. Preliminary conclusions

As a matter of interest of this study, fan tonal noise generation was investigated in a sub-sonic fan stage in the presence of inflow distortions. The main effect of the investigated inflow distortions seem to be a modulation of the RSI. This hypothesis is based on the observed major excitation of the modes adjacent to the Tyler-Sofrin modes. The second tonal noise source of interest was the interaction of the mean flow profile with the rotor. For the analysis of this noise source mechanism analytical models are available in the literature. The results show no clear relevance of this noise source. However, the excited mode spectra of the strongly distorted cases with 50% fence height plausibly look like this mechanism is relevant for the excitation of co-rotating upstream propagating modes. This noise source is expected to be stronger at high blade tip Mach numbers or with small blade counts. The overall sound power level is reduced for some inflow distortion at specific BPF harmonics. This opens new possible design spaces for distortion tolerant fans, if this effect could be predicted based on the expected inflow distortion.

The next step comprises the simulation of the presented test cases using an analytical approach to calculate the tonal noise from inflow-distortion-rotor interaction. Further work is necessary to understand the modulation of the Tyler-Sofrin modes and to create a prediction model for the broader mode spectra excited by the distorted Rotor-Stator interaction. Extensive hot wire measurements downstream the fan by means of hot-wire are planned in order to assess the periodic changes of the rotor wakes. Additionally, further research will be conducted to assess the effect of distorted mean flow on refracted mode shapes.

## References


[1] Tapken, U. et al. "Fan test rig for detailed investigation of noise generation mechanisms due to inflow disturbances". In: *AIAA AVIATION 2021 FORUM*. 2021.

[2] Tyler, J. M. and Sofrin, T. G. "Axial Flow Compressor Noise Studies". In: *SAE Technical Paper* (Jan. 1962).

[3] Schade, S., Jaron, R., Moreau, A., and Guérin, S. "Mechanisms to reduce the blade passing frequency tone for subsonic low-count OGV fans". In: *Aerospace Science and Technology* 125 (2022). SI: DICUAM 2021, p. 107083.

[4] Gunn, E. J. and Hall, C. A. "Aerodynamics of Boundary Layer Ingesting Fans". In: *Turbo Expo: Power for Land, Sea, and Air*. Vol. Volume 1A: Aircraft Engine; Fans and Blowers. June 2014.

[5] Kim, H. D., Perry, A. T., and Ansell, P. J. "A review of distributed electric propulsion concepts for air vehicle technology". In: *2018 AIAA/IEEE Electric Aircraft Technologies Symposium (EATS)*. IEEE. 2018.

[6] Kobayashi, H. and Groeneweg, J. F. "Effects of inflow distortion profiles on fan tone noise". In: *AIAA Journal* 18.8 (1980), pp. 899–906.

[7] Staggat, M. "Modellierung und Prognose des Grenzschicht-Rotor-Interaktionsschalls für integrierte Triebwerke". PhD thesis. Technische Universit"at Berlin, 2021.

[8] Daroukh, M., Polacsek, C., and Carini, M. "Acoustic Assessment of BLI Effects on Airbus Nautilius Engine Integration Concept - Part I: Noise Generation". In: *28th AIAA/CEAS Aeroacoustics 2022 Conference*. 2022.

[9] Le Garrec, T., Polacsek, C., Chelius, A., Daroukh, M., and François, B. "Tone Noise Predictions of a Full-Scale UHBR Engine at Approach Condition with Inflow Distortion Effects". In: *25th AIAA/CEAS Aeroacoustics Conference*. Delft, The Netherlands, May 2019.

[10] Petrosino, F., Barbarino, M., and Staggat, M. "Aeroacoustics Assessment of an Hybrid Aircraft Configuration with Rear-Mounted Boundary Layer Ingested Engine". In: *Applied Sciences* 11.7 (2021).

[11] Caldas, L., Klähn, L., Meyer, R., and Tapken, U. "Measurements of fan inflow distortion noise generation in a low speed fan – part I: aerodynamic analyses". In: *28th AIAA/CEAS Aeroacoustics Conference*. Southampton, UK, June 2022.

[12] Klähn, L., Caldas, L., and Tapken, U. "Measurements of fan inflow distortion noise generation in a low speed fan - part II: acoustic analyses". In: *28th AIAA/CEAS Aeroacoustics Conference, Southampton, UK*. 2022.

[13] Behn, M., Pardowitz, B., and Tapken, U. "Separation of tonal and broadband noise components by cyclostationary analysis of the modal sound field in a low-speed fan test rig". In: *International Conference of Fan Noise, Aerodynamics, Applications and Systems*. 043. Darmstadt, Germany, Apr. 2018.

[14] Spitalny, M. and Tapken, U. "Radial Mode Analysis of Ducted Sound Fields with Sensor Rakes and Wall Flush Sensor Arrays under Consideration of a Radial Flow Profile". In: *22nd AIAA/CEAS Aeroacoustics Conference*. AIAA 2016-3037. May 2016.